

**LINEAR ELASTIC FRACTURE MECHANICS (LEFM) APPROACH TO FATIGUE
LIFE PREDICTION (OR EARTHQUAKE PREDICTION) ALONG THE NAF, SAF
AND EAF ZONES**

UĞUR KURAN, Geophysicist (Ret'd)

**The Ministry of Public Works & Settlement
General Directorate of Disaster Affairs
Earthquake Research Department, Ankara, TÜRKİYE**

In order to permit the development of an adequate linear elastic fracture mechanics approach to the earthquake prediction studies, K_2 (the stress intensity factor for mode-II deformation or shear modes) and crack growth rate (da/dN) must be available for the NAF zone. The stress intensity parameter K describes the stress situation at the tip of an existing crack which, in turn, is a controlling factor for fatigue crack growth. As a result, the stress intensity concept provides a realistic parameter which can be used to evaluate and describe the fatigue characteristics of crustal structure. Within the limits of linear elastic fracture mechanics, the driving force of crack propagation is known to be a function of the applied stress intensity, K , which has the general form:

$$K = \sigma \sqrt{\pi a} \cdot f\left(\frac{a}{W}\right) \quad (1)$$

in which σ is the far field stress resulting from cyclic tidal load [Kuran, 1979]; $f(a/W)$ = the finite width correction and a = the half crack length.

The stress intensity factor for mode II deformation (K_2) along the NAF zone may be expressed in the following form:

$$K_2 = \sigma \sin \alpha \cdot \cos \alpha \sqrt{\pi \cdot a} \left[1.146 - 4.247 \left(\frac{a}{W}\right) + 41.801 \left(\frac{a}{W}\right)^2 - 148.44 \left(\frac{a}{W}\right)^3 + 193.719 \left(\frac{a}{W}\right)^4 \right] \quad (2)$$

Where the factor in parenthesis indicates the effect of the final width, and the values of the coefficients of these fourth-degree polynomials were obtained from the tangent formula and also given in Table 1, Fig.1. The angle between the cyclic loading direction of the tidal load and the shear zone (i.e. 1939 fault break) is denoted by α (π is introduced for convenience), $\sigma \sin \alpha \cdot \cos \alpha = 4.51$ Ksi. [Kuran.2000] The generalized fatigue crack growth law the form of

$$\frac{da}{dN} = A \cdot K^n \quad (3) \quad \text{Paris, 1962, Paris and Erdoğan, 1963, Paris.1964.}$$

where $K = K_{\max} - K_{\min} = \sigma_{\max} (\pi a)^{1/2} - \sigma_{\min} (\pi a)^{1/2}$ and σ_a is the cyclic stress amplitude, n is the slope of the $\log(da/dN)$ versus $\log K$ curve and A (or C) is an empirical constant determined from the data (i.e. da/dN axis intercept). The component of K in Eq.3 often being near four (i.e. "fourth-power law").

The theory of Paris is based on the following arguments: The crack is considered to be an elliptic hole in the infinite sheet with a zero minor axis and the major axis equal to the crack length. Paris, also argues that the crack rate is fully determined by local stresses around the crack tip, and since K determines the stress field in the tip region this parameter and only this governs the rate of crack growth. Paris suggested that K should be applicable to random load if S_{rms} (the root-mean-square stress range of the random load history) substituted in above equation (Eq. 3) Paris, 1964.

Determination of da/dN versus K_2 data

Table 1 gives the summary of Fracture Parameters and enables us to calculate crack growth rates and hence total life. In order to express the raw field data $2a_1, (a_1 - a_2)$ and N in terms of fracture mechanics, the data were converted to the form of crack-growth rate, da/dN , versus cyclic stress intensity factor for mode-II as shown in Table 1. The crack growth rate were determined from Column 1 and 4, and crack-growth-rate expressed in 10^3 Inch/ cycle or [year]. Where $2(a_1 - a_2)$ in Table1 [Fig.1] are the fatigue cracks which measure the center to center distance of the ellipses shown in Fig.2.

There is no simple relationship between the rate of crack growth and stress intensity factor that holds precisely over the entire range (please see 1912 event), but as indicated in the Figure (3) the da/dN versus K_2 data fall within a narrow scatter band between 1894 and 1944. The rate of fatigue crack growth increases with increasing stress intensity factor. The slope of this line is such that the rate of propagation is proportioned to $\sigma \cdot \sin \alpha \cdot \cos \alpha \sqrt{\pi a} f(a/W)$ raised to the fifth power.

The best fit straight line from a linear regression of $\log da/dN$ versus $\log K_2$ takes the form of

$$\frac{da}{dN} = 9.37 \cdot 10^{-17} (K_2)^{4.726}, \text{STD. ERROR}(0.3144) \quad (4a)$$

For the lower-scatter-band Eq.3 takes the form of

$$\frac{da}{dN} = 2.75 \cdot 10^{-16} (K_2)^{4.5997}, \text{STD.ERROR}(0.0439) \quad (4b)$$

The crack rate $(da_1/dN_1 + da_2/dN_2)/2$ was calculated as a linear average between two successive “a”- values in the Table I.

For the lower-scatter-band of $(\frac{da_1}{dN_1} + \frac{da_2}{dN_2}) / 2$ versus K_2 takes the form of

$$\frac{da}{dN} = 2.8973.10^{-14} (K_2)^{4.26} \quad (4c)$$

Note that the Paris law exponent is close to 4.

Failure Time Prediction (or Prediction of macro-crack propagation):

The Paris-Erdoğan crack growth rate equation $da/dN = A (K)^n$ is often a reasonable-expression for region II (or Region B ,Parker 1981,p.125) crack growth behavior. The number of cycles to propagate a crack from initial size a_i (112.5 km, initial crack length for the year 1894) to some size a_f (442.5 ,559.5 ,681.5 km-final crack lengths for the years of 1939, 1943 and 1944 respectively are obtained by integrating the Paris equation.

$$N = \int_{a_f}^{a_i} \frac{1}{A(K)^n} da \quad (5)$$

The average period required to initiate the first fatigue failure may be obtained from Eq. 6.

$$N = \frac{1}{A \cdot Q^n \pi^{n/2} \sigma^n} \times \frac{a_i^{(1-n/2)} - a_f^{(1-n/2)}}{n/2 - 1} \quad \text{Parker (1981)} \quad (6)$$

This equation is not correct if n is equal to 2.

Once the Paris-Erdoğan crack growth rate equation of the type Eq.4 is obtained for the NAF zone, it is a relatively simple matter to use the fracture mechanics approach for time prediction.

In order to use equation 6 for the failure time prediction, it will be necessary to determine Q-value (Configuration correction factor, Parker, 1981(p.123) Q-value is determined from the same equation by substituting the values: $A=9.3667.10^{-7}$, $1-n/2 = -1.363$, $N= 50$ (1944-1894), $\pi^{2.363}$ and $\sigma^n = (4.51)^{4.7260}$, $a_i^{1-n/2} = 7.9815.10^{-10}$ and solving Q from

$$Q_n = \frac{1}{9.3667 \cdot 10^{-17} \times 50 \times 3.14^{2.363} \times (4.51)^{4.7260}}$$

$$\times \frac{[112.5]^{-1.363} - [681.5]^{-1.363}}{-1.363} \quad (7)$$

The Q-value may be extracted immediately as $Q=1.49884$. It will be assumed that the variation in Q is small for the whole range of crack lengths up to a_f , and we shall assume a constant value, $Q=1.5$, in order to predict life-expectancy (Note that a_i and a_f values should be converted to inches prior to use of Eq.7). The accurate prediction of the life time of a complex crustal structure (or the safe living for people along the NAF zone) can be calculated from Eq.6 in the following way:

For the Dec.26, 1939 Erzincan earthquake;

$$\begin{aligned} a_i &= 112.5 \text{ km} \\ a_f &= 442.5 \text{ km} \\ Q &= 1.49884 \quad T_f = 1894 + 46.237 = 1940.23 \end{aligned}$$

Where, T_f is the time of failure (main shock).

For the Nov.26, 1943 earthquake;

$$\begin{aligned} a_i &= 112.5 \text{ km} \\ a_f &= 559.5 \text{ km} \\ Q &= 1.49884 \quad T_f = 1894 + 48.552 = 1942.552 \end{aligned}$$

For the Feb.1, 1944 earthquake;

$$\begin{aligned} a_i &= 112.5 \text{ km} \\ a_f &= 681.5 \text{ km} \\ Q &= 1.49884 \quad T_f = 1894 + 50 = 1944 \end{aligned}$$

Thus, calculation of the fatigue-macro crack propagation life is possible, using the da/dN - K_2 curve appropriate to the three-dimensional crustal structure. From the preceding analysis, it is evident that, once the value of Q has been determined time prediction may be achieved.

Examination of the Eq.4c $(da_1/dN_1 + da_2/dN_2)/2$ "Geometric Mean"-Parker, 1981 also indicates that a life of 50 cycles should occur when $Q=1.22$. Assuming that $A = 2.8973 \cdot 10^{-14}$, $a_i = 112.5 \text{ km}$, $1-n/2 = -1.13$, computation of crack growth from $a_i = 112.5 \text{ km}$, to $a_f = 442.5 \text{ km}$ (1939), give the following results: Eq.4c. $a_i = 112.5 \text{ km}$, $a_f = 442.5 \text{ km}$, $N = 45.275 + 1894 = 1939.28$, and Eq.4.c. $a_i = 112.5 \text{ km}$, $a_f = 559.5 \text{ km}$, $N = 48.124 + 1894 = 1942.123$ and Eq.4.c; $a_i = 112.5 \text{ km}$, $a_f = 681.5$, $N = 50 + 1894 = 1944$. Thus, it appears that life prediction (Eqs. 4a and 4c) within this accuracy may be the best that can be achieved.

From the preceding analysis, it is evident that the linear fracture mechanics approach may be used to approximate fatigue crack propagation behavior in crustal structure.

Prediction of Crustal Structure Life by Application of Fatigue Crack Growth Knowledge Along the EAF Zone

The study of the East Anatolian Fault zone shows that major earthquake sequences associated with faulting have been occurring in the zone since historical times. One of the most interesting recent sequences is that of 1822-1905. During that period at least five destructive magnitudes occurred along the NAF zone (Ambraseys, 1989; Seymen and Aydin, 1972).

Figure 5 shows the fault breaks associated with three of the larger earthquakes that occurred in the zone since 1822. According to Ambraseys (1989), the earthquake of 1822 and 1872 were associated with faulting in the Afrine and Amik fracture zones. He suggested that these and earlier major events in this region are a southward extension of the EAF zone. Three shocks which took place in the vicinity of the Amanos fault in 1796(6.6), 1822(7.4) and 1872(7.2) caused considerable damage in all areas of Hatay province and the Syria. Repeat but moderate size earthquakes along the Misis fault [524,528,561,] are very characteristic especially when towns are located within the circular shape yield zone. One of the best and recent examples is the Parkfield-Cholame main shocks of 1857, 1901, 1922, 1934 and 1966. Parkfield and Cholame are located along the radius of circular yield zone which is in the direction of the maximum shear zone of the San Andreas Fault system. Therefore, it is concluded that the ancient provinces Issos, Karatepe, Bahçe, and Anazarva are also lying along the diameter of circular yield zone in ellipse No. 7. This segment is commonly known as "the Misis fault" in this region {similar to the Hayward fault in California}. From available evidence, it is concluded that both of the fracture [the Amanos and Misis fault zones] were arrested by the ellipse No.7. The predicted maximum extension of the fault break shown by the zig zag lines between ellipse No.6 and 7 (~485 km). Kuran 2000.

The East Anatolian Fault Zone is a transform fault boundary between the Anatolian Block to the NW and the Arabian-African plates to the SE (Doyuran et al., 1989, p.16). The East Anatolian Fault is a relatively simple and easily followed break throughout most of this segment but southwest from Maraş, it splits into a number of branches.

It is clear all instrumentally located events occurring in the Gulf of Iskenderun between 1951-1966 provide evidence of a terminal of the branching fault which lies between Kahramanmaraş province and the Gulf of Iskenderun. If this interpretation is correct, the EAF splays out into the three section from the Kahramanmaraş junction a) The Amanos fault section, b) The Misis section and c) The Gulf of Iskenderun fault section.

The method employing the K-parameter description of elastic stress intensity in crustal structure therefore, will be used two ellipses along the Amanos tectonic zone rather than the Misis fault.

The second major activity took place in the center of the ellipse is No.7 in 1872. The approximate fault break associated with these events is estimated to be about 150 km. These results are based on the identification and location of the two larger events and also the extent of damage and felt areas (Ambraseys, 1989). It is interesting to note that the circular shape yield zones in Fig.(4) are the most likely places for the generation of moderate size earthquakes which took place in 1893 and 1905. The time prediction [estimated date] can be determined by the method explained above by the use of a FORTRAN program, so that E.Q.4c fits the actual date in the best possible way. [Durmuşoğlu, Ö. 2000].

Application of this program for time prediction was made by the use of the equation 4c for the North Anatolian [Fig.4,11], East Anatolian [Figs.5,6,7] and SAF zones [Figs.8,9,10]. For a high quality short-term earthquake prediction, however it is necessary to investigate cyclic-strain-softening {Kuran,1975,1977,1979,2000 and ,2001} which was dominant three days before the catastrophic earthquakes in The 1999 İzmit and Bolu which was obtained by the use of tilt meter .

Sharp increase in deformation rate, which occur three days after the total solar eclipse, was quite remarkable. Due to the total eclipse increase in the daily tidal stress was about 18 percent. Prior to the occurrence of the main shock peak to peak amplitude of the diurnal tidal cycle decreased about 58 percent. The decrease in deformation resistance with cyclic loading is known as deformation (or strain) softening. The softening is characterized by a rapid increase in strain rate under cyclic applied stress range. The rate of cyclic strain softening (or strain weakening), $d\varepsilon/dt$, is considered to be the slope of the strain-time diagram for gradually incremental cyclic tidal loading. This effect is seen more convincingly during the course of laboratory experimental studies, also before a rock burst which took place in the Zigana highway tunnel in 1977, and also long before the Tottori earthquake of 1943 [Hagiwara, 1975].

Concluding Remark

Fatigue Crack Propagation in crustal structures is a very important problem at the present stage of earthquake prediction technique development. It is therefore of great importance to have accurate methods in forecasting technique for time prediction of a destructive earthquake. Through theoretical and experimental research carried out at the Imperial College [Geophysics Department], University of London and the Earthquake Research Department in Ankara, it has been possible to make some contributions to the solution of the said problem. Kuran, 1975.

On the theoretical side, the stress/strain/time phenomena of crustal material have been investigated. On the experimental side, many crack propagation tests on granite, andesite and sandstone rocks have been carried out. The method employing the K-parameter description of elastic stress intensity in material surrounding the tip of a crack has been used during the course of this study. It seems reasonable that results of laboratory studies may be extended to apply to seismic activity, particularly micro-earthquake phenomena and also provided clear understanding of strain-step mechanisms operative at high stresses.

Long term macro and micro earthquake studies, including historical seismicity provide important basic information on the discontinuous fatigue- crack growth process along the active faults. Through the use of fracture mechanics, several examples of prediction of the occurrence time of earthquakes are given, including detailed predictions for, the SAF and EAF zones. It is concluded that the Linear Elastic Fracture Mechanics approach may be used to approximate fatigue crack propagation behavior in crustal structure, it has been possible to make some contributions to the solution of the said problem.

REFERENCES

- Albrecht, Pedro, Kentaro Yamada, 1977.** Rapid Calculation of Stress Intensity Factors. Proc. of the ASCE. Journal of the structural division, Vol.103, No.ST2.
- Ambraseys, N.N. 1989.** Temporary Seismic quiescence: SE Turkey; Geophys. J.96, 311-331.
- Durmuşoğlu, Özcan. 2000., Private Communication.**
- Hagiwara, T., 1975.** Recent Research on Earthquake Prediction. Fifth European Conference on Earthquake Engineering .İstanbul
- Kuran, Uğur, 1975.,** An experimental investigations of cyclic stress-strain relation and fatigue crack propagation in crustal material, PhD theses. Geophysics Dept. Imperial College –London.
- Kuran, Uğur, 1977.,** Stress-deformation Deformation-time phenomena in the Zigana Highway Tunnel and Landslide Area., Jeofizik, Pub. of Geoph. Assoc. of Turkey. No.2,3, Vol.VI, PP.5-28
- Kuran, Uğur, 1979.** Stress/deformation/time phenomena in the landslide areas of Yeşildere. Bulletin of the Geological Congress of Turkey, 1, 1979.
- Kuran, Uğur, 1979.** Fatigue-crack-propagation within the earth's crust due to cyclic tidal loading and earthquake prediction along the San Andreas and North-Anatolian Fault zones. Jeofizik, Vol.VIII, No.3, pp.75-123.
- Kuran, U. 2000.** World-Wide Comprehensive Earthquake Prediction Studies by the use of LEFM criteria. Earthquake Research Department, Ankara. Unpublished Manuscript
- Kuran, Uğur, 2001,** Microzonation Studies in Avcılar, İstanbul., Earthquake Research Depth. Ankara
- Paris, P., 1962.** The Growth of Cracks due to variations in Load. Doctoral Dissertation (Lehigh University).
- Paris, P., and F. Erdoğan, 1963.** "A Critical Analysis of Crack Propagation Laws". J.Bas. Engrg. Trans. Am. Soc. Mech. Engrs. Series D. Vol.85.
- Paris, P.C., 1964.** The fracture Mechanics Approach to Fatigue. Proc. of the 10th Sagamore Arm. Materials Research Conference. Syracuse University Press.
- Parker, A.P., 1981.** The Mechanics of Fracture and Fatigue. "An Introduction" E and FN SPON LTD.

FIG 1. SUMMARY OF FRACTURE PARAMETERS ALONG THE NAF ZONE (W=1363 km).

dN (Years)	(2a) 10 ⁶ mm	aav 10 ⁶ mm	2(a ₁ -a _i) 10 ⁶ mm	da/dN 10 ³ inch/cycle	Q	a/W	k ₂ [*] 10 ³ ksi /inch	(da ₁ dN ₁ +da ₂ dN ₂)/2 10 ³ inch/cycle
1509-1894	225	112.5	225	11.504	1.006	0.0825	16.924	11.504
		205	370	404.636	1.047	0.150	23.777	331.110
1894-1912	595				1.1066	0.218	30.274	650.698
		370	290	211.431	1.1555	0.271	35.254	647.904
1912-1939	885				1.246	0.325	41.573	645.231
		501	234	1176.094	1.3968	0.368	49.598	3134.685
1939-1943	1119				1.679	0.411	62.992	5624.142
		620.5	244	26566	2.191	0.455	86.575	77012
1943-1944	1363					0.5	125.250	148399.64

$$k_2^* = 0.5 \sin(\theta) \cos(\theta) / \pi a \left(1.146 - 4.247(a/W) + 41.801(a/W)^2 - 148.441(a/W)^3 + 193.719(a/W)^4 \right)$$

Fig 2 Time Prediction

$b=185.0000$
 $c=145.0000$
 $d=117.0000$
 $e=122.0000$
 $W=1360.0000$

The Date of Final Destructive Earthquake=1944.0000
 Initial Crack Length(km)=112.5000

Date (Year)		Est. Date		Difference
1894	$1 - (n/2)$ $a_i - af_1(W/2)$	1894	-0.0	
1912	$1 - (n/2)$ $a_i - af_2(a_i+b)$	1932	-20.4	
1939	$1 - (n/2)$ $a_i - af_3(a_i+b+c)$	1939	-0.3	
1943	$1 - (n/2)$ $a_i - af_4(a_i+b+c+d)$	1942	0.9	
1944	$1 - (n/2)$ $a_i - af_5(a_i+b+c+d+e)$	1944	-0.0	
1944	$1 - (n/2)$ $a_i - af_6(af_5 - af_1)$	1944	0.0	

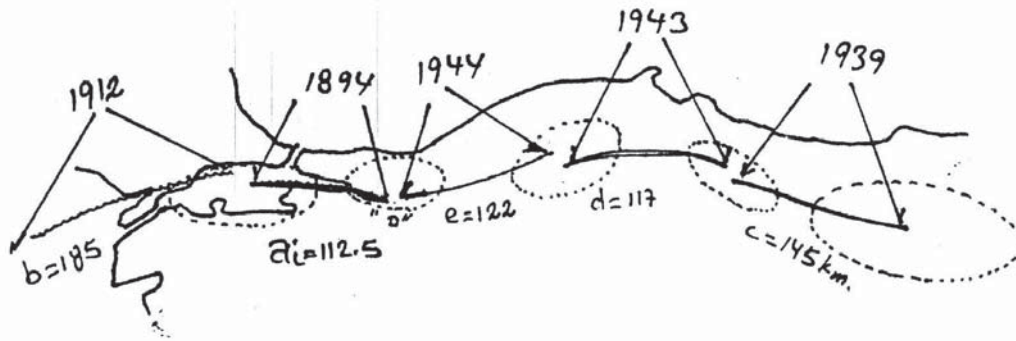


Fig 3. RELATIONSHIP BETWEEN THE STRESS INTENSITY AND CRACK PROPAGATION RATE FOR MODE-II ALONG THE NAF ZONE

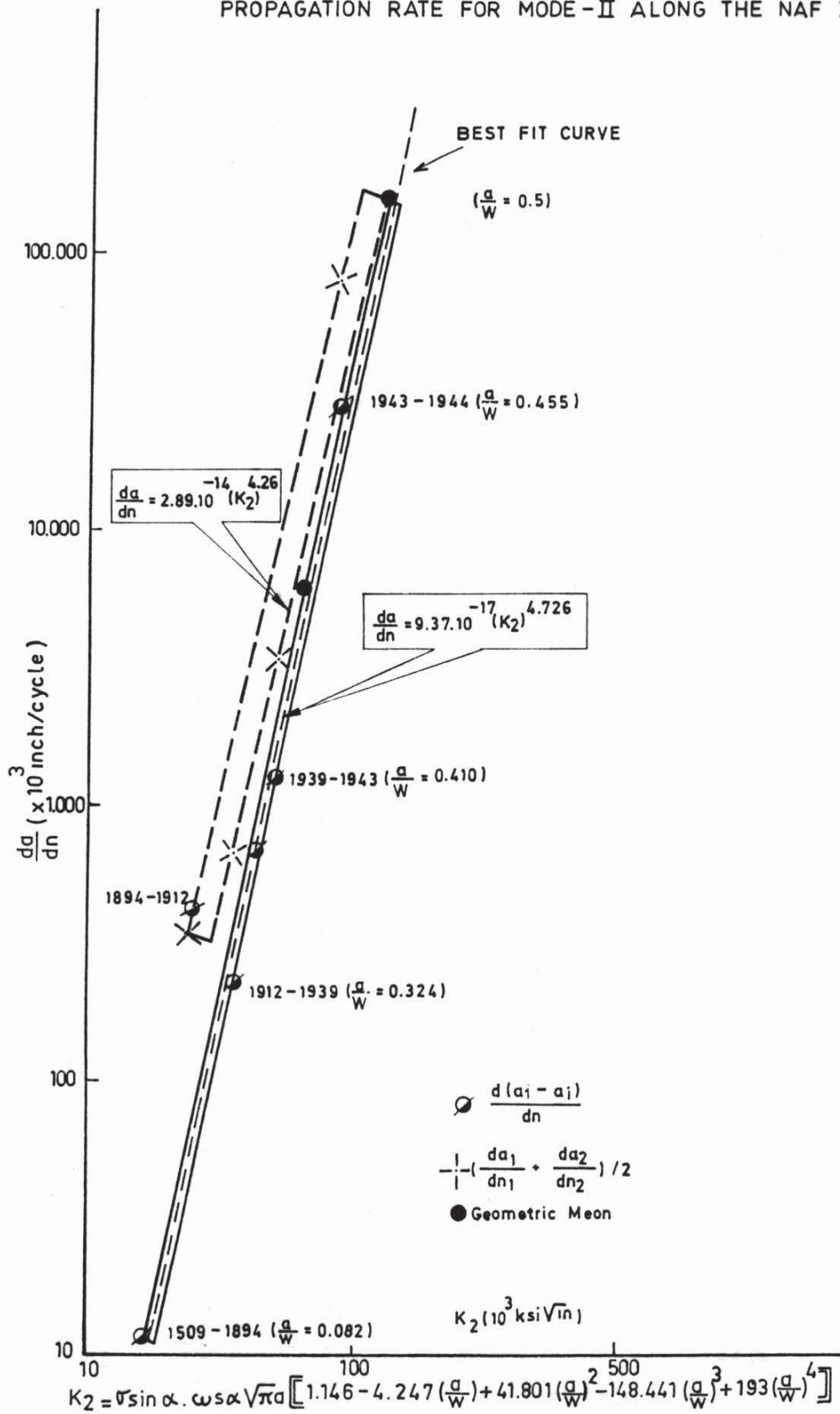


FIG.4 Time Prediction

b=55.0000
 c=12.5685
 d=13.0105
 e=12.5685
 W=290.0000

The Date of Final Destructive Earthquake=1939.0000
 Initial Crack Length(km)=20.3500

Date(Year)		Est. Date Difference	
1585	$\frac{1-(n/2)}{a_1} - \frac{(1-n/2)}{af_1(W/2)}$	1585	-0.0
1888	$\frac{-(n/2)}{a_1} - \frac{(1-n/2)}{af_2(a_i+b)}$	1892	-3.7
1909	$\frac{1-(n/2)}{a_i} - \frac{(1-n/2)}{af_3(a_i+b+c)}$	1906	2.3
1916	$\frac{1-(n/2)}{a_i} - \frac{(1-n/2)}{af_4(a_i+b+c+d)}$	1917	-1.2
1929	$\frac{1-(n/2)}{a_i} - \frac{(1-n/2)}{af_5(a_i+b+c+d+e)}$	1925	3.8
1939	$\frac{1-(n/2)}{a_i} - \frac{(1-n/2)}{af_7(af_5-af_1)}$	1939	0.0

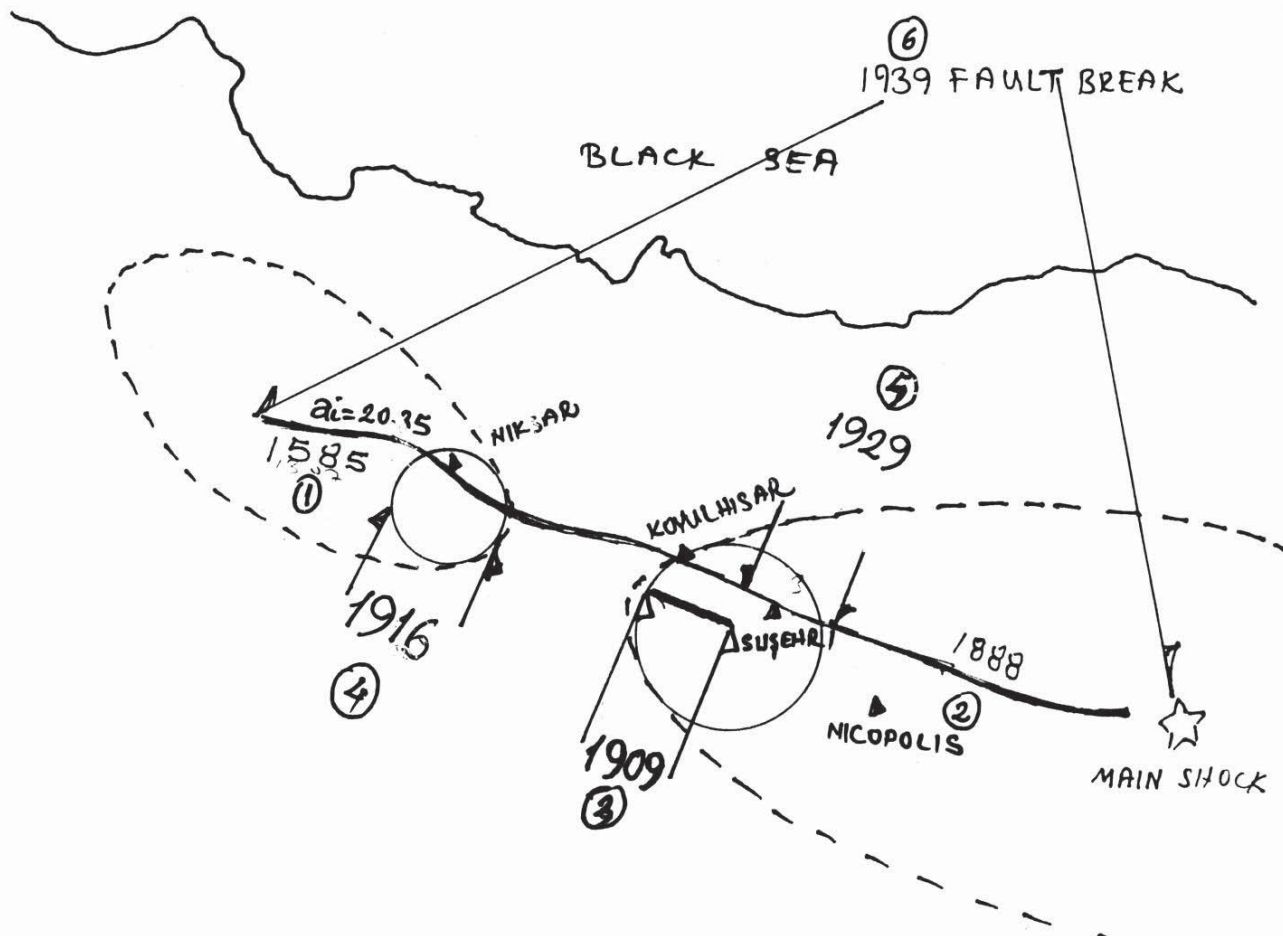


FIG.5 Time Prediction

b=37.0000
 c=75.0000
 d=34.0000
 e=19.0000
 f=19.0000
 W=494.0000

The Date of Final Destructive Earthquake=1919.0000
 Initial Crack Length(km)=19.0000

Date(Year)			Est. Date	Difference
0	$1 - (n/2)$ ai	$(1 - n/2)$ - af1(W/2)	1513	-1513.5
1822	$1 - (n/2)$ ai	$(1 - n/2)$ - af2(ai+b)	1816	5.9
1872	$1 - (n/2)$ ai	$(1 - n/2)$ - af3(ai+b+c)	1894	-22.2
1874	$1 - (n/2)$ ai	$(1 - n/2)$ - af4(ai+b+c+d)	1905	-31.3
1893	$1 - (n/2)$ ai	$(1 - n/2)$ - af5(ai+b+c+d+e)	1910	-16.7
1905	$1 - (n/2)$ ai	$(1 - n/2)$ - af6(ai+b+c+d+e+f)	1913	-8.1
1919	$1 - (n/2)$ ai	$(1 - n/2)$ - af7(af6-af1)	1916	3.5

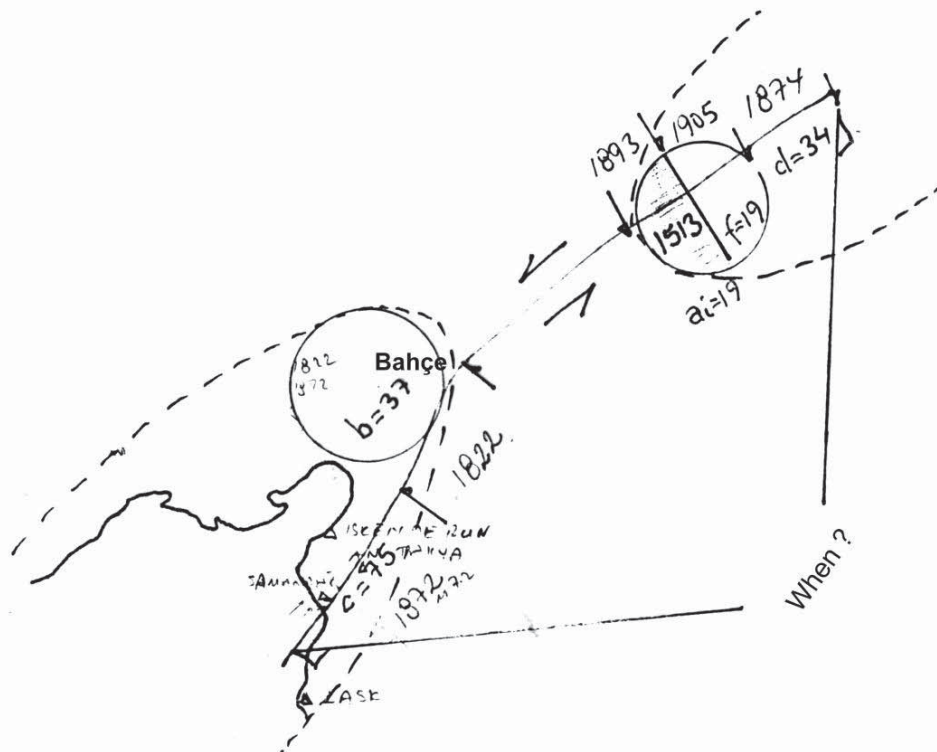


FIG.6 Time Prediction

b=37.0000
 c=75.0000
 d=34.0000
 e=19.0000
 f=19.0000
 W=494.0000

The Date of Final Destructive Earthquake=1513.0000
 Initial Crack Length(km)=19.0000

Date (Year)			Est. Date	Difference
0	$1 - (n/2)$ ai	$(1 - n/2)$ af1(W/2)	1107	-1107.5
0	$1 - (n/2)$ ai	$(1 - n/2)$ af2(ai+b)	1410	-1410.1
0	$1 - (n/2)$ ai	$(1 - n/2)$ af3(ai+b+c)	1488	-1488.2
0	$1 - (n/2)$ ai	$(1 - n/2)$ af4(ai+b+c+d)	1499	-1499.3
0	$1 - (n/2)$ ai	$(1 - n/2)$ af5(ai+b+c+d+e)	1504	-1503.7
0	$1 - (n/2)$ ai	$(1 - n/2)$ af6(ai+b+c+d+e+f)	1507	-1507.1
1513	$1 - (n/2)$ ai	$(1 - n/2)$ af7(af6-af1)	1510	3.5

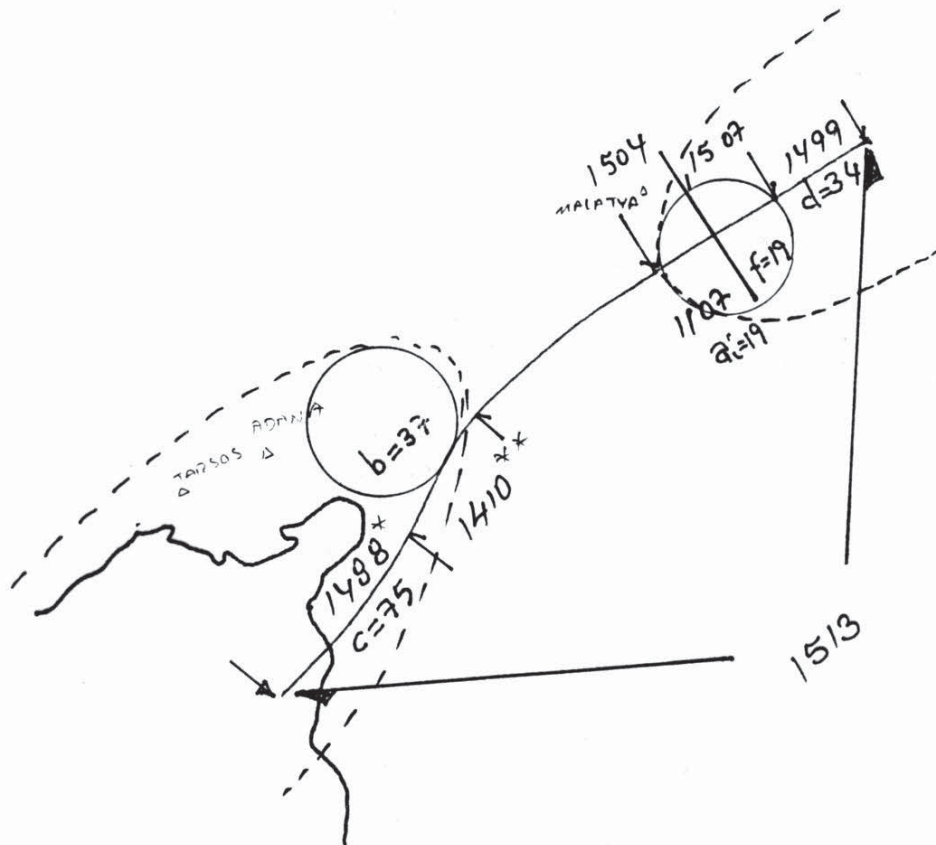


Fig 7. Time Prediction (HAZAR LAKE-OFF SÜVEYDIYE

b=37.0000
 c=75.0000
 d=34.0000
 e=19.0000
 f=19.0000
 W=494.0000

The Date of Final Destructive Earthquake=458.0000
 Initial Crack Length(km)=19.0000

Date(Year)			Est. Date	Difference
53	$1 - (n/2)$ ai	$(1 - n/2)$ - af1(W/2)	52	0.5
341	$1 - (n/2)$ ai	$(1 - n/2)$ - af2(ai+b)	355	-14.1
434	$1 - (n/2)$ ai	$(1 - n/2)$ - af3(ai+b+c)	433	0.8
?	$1 - (n/2)$ ai	$(1 - n/2)$ - af4(ai+b+c+d)	444	
?	$1 - (n/2)$ ai	$(1 - n/2)$ - af5(ai+b+c+d+e)	449	
?	$1 - (n/2)$ ai	$(1 - n/2)$ - af6(ai+b+c+d+e+f)	452	
?	$1 - (n/2)$ ai	$(1 - n/2)$ - af7(af6-af1)	455	

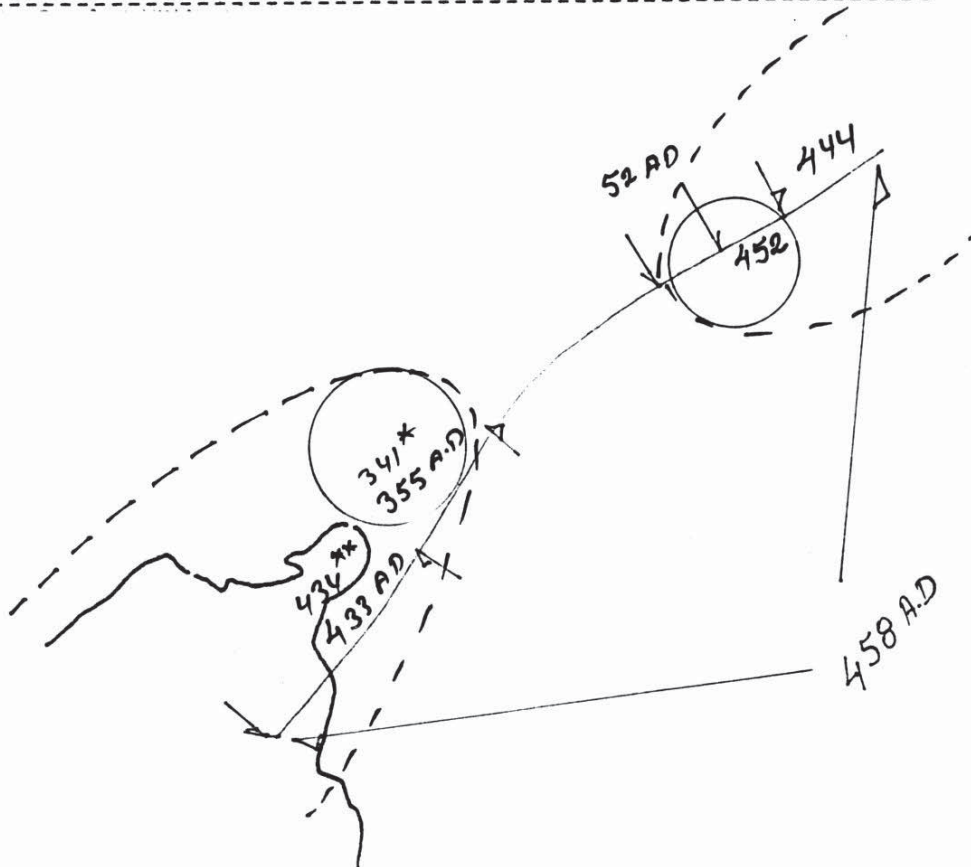


Fig 8. Time Prediction (SAF)

b=51.7000
 c=80.0000
 d=68.5000
 e=18.5000
 W=676.0000

The Date of Final Destructive Earthquake=1458.0000
 Initial Crack Length(km)=18.5000

Date (Year)			Est. Date	Difference
0	$\frac{1-(n/2)}{a_i}$	$\frac{(1-n/2)}{af1(W/2)}$	1032	-1032.3
0	$\frac{1-(n/2)}{a_i}$	$\frac{(1-n/2)}{af2(a_i+b)}$	1377	-1376.6
0	$\frac{1-(n/2)}{a_i}$	$\frac{(1-n/2)}{af3(a_i+b+c)}$	1433	-1433.1
0	$\frac{1-(n/2)}{a_i}$	$\frac{(1-n/2)}{af4(a_i+b+c+d)}$	1447	-1447.5
0	$\frac{1-(n/2)}{a_i}$	$\frac{(1-n/2)}{af5(a_i+b+c+d+e)}$	1450	-1449.8
1458	$\frac{1-(n/2)}{a_i}$	$\frac{(1-n/2)}{af6(af5-af1)}$	1458	0.0

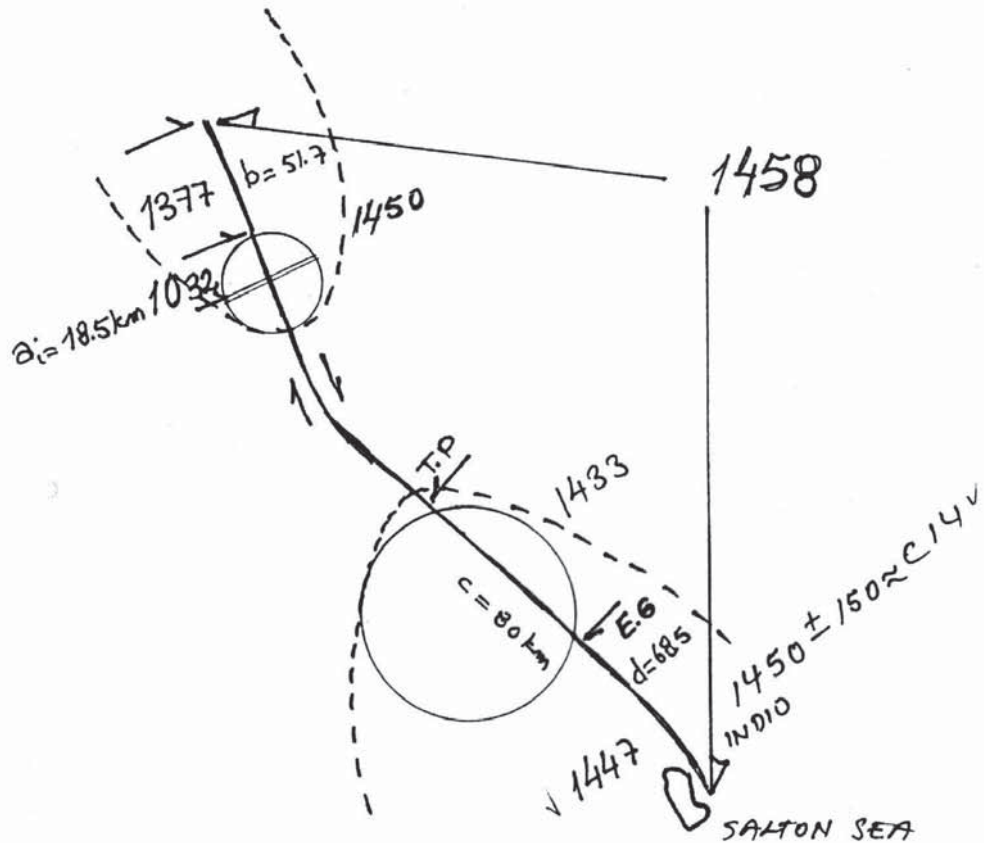


Fig 9. Time Prediction (SAF)

b=51.7000
c=80.0000
d=68.5000
e=18.5000
f=18.5000
W=676.0000

The Date of Final Destructive Earthquake=1857.0000
 Initial Crack Length(km)=18.5000

Date (Year)			Est. Date	Difference
0	$\frac{1-(n/2)}{a_i}$	$\frac{(1-n/2)}{af_1(W/2)}$	1431	-1431.3
0	$\frac{1-(n/2)}{a_i}$	$\frac{(1-n/2)}{af_2(a_i+b)}$	1776	-1775.6
1812	$\frac{1-(n/2)}{a_i}$	$\frac{(1-n/2)}{af_3(a_i+b+c)}$	1832	-20.1
0	$\frac{1-(n/2)}{a_i}$	$\frac{(1-n/2)}{af_4(a_i+b+c+d)}$	1846	-1846.5
0	$\frac{1-(n/2)}{a_i}$	$\frac{(1-n/2)}{af_5(a_i+b+c+d+e)}$	1849	-1848.8
0	$\frac{1-(n/2)}{a_i}$	$\frac{(1-n/2)}{af_6(a_i+b+c+d+e+f)}$	1851	-1850.8
1857	$\frac{1-(n/2)}{a_i}$	$\frac{(1-n/2)}{af_7(af_6-af_1)}$	1855	2.0

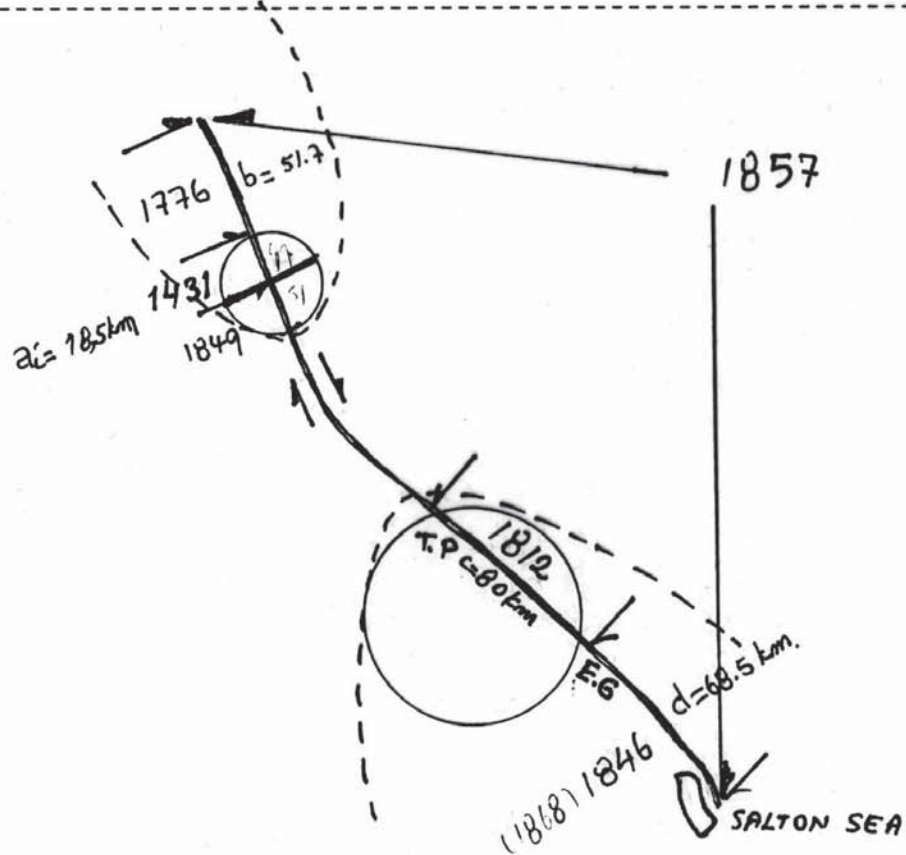


Fig 11. Time Prediction(SAF)

b=14.3500
 c=30.6500
 d=26.5000
 e=0.0000
 W=432.0000

The Date of Final Destructive Earthquake=2187.0000
 Initial Crack Length(km)=33.5000

Date(Year)		Est. Date	Difference
1989	$1 - (n/2)$ ai - af1(W/2)	1988	0.6
0	$1 - (n/2)$ ai - af2(ai+b)	2063	-2063.4
0	$1 - (n/2)$ ai - af3(ai+b+c)	2128	-2128.1
0	$1 - (n/2)$ ai - af4(ai+b+c+d)	2152	-2152.3
0	$1 - (n/2)$ ai - af5(ai+b+c+d+e)	2152	-2152.3
2187	$1 - (n/2)$ ai - af6(af5-af1)	2187	-0.0

